Drug Nanocrystals: Theoretical Background of Solubility Increase and Dissolution Rate Enhancement

D. Hasa,[a] B. Perissutti,[a] D. Voinovich,[a] M. Abrami,[b] R. Farra,[b] S. M. Fiorentino,[b] G. Grassi,[c] and M. Grassi[b,*]

[a]Department of Chemical and Pharmaceutical Sciences, University of Trieste, Piazzale Europa 1, I-34127, Trieste, Italy

[b]Department of Engineering and Architercture, Via A. Valerio 6/A, I-34127, Trieste, Italy

[c]Department of Life Sciences, Cattinara University Hospital, Strada di Fiume 447, I-34149, Trieste, Italy

doi: 10.15255/CABEQ.2013.1835

Original scientific paper
Received: July 1, 2013
Accepted: July 25, 2014

The peculiar higher solubility of drug nanocrystals compared to macrocrystals appeals to the pharmaceutical field. Indeed, until now, about 70 % of the potential drug candidates are discarded due to low bioavailability related with poor solubility in water. Since a modern and efficient design strategy for nanocrystal-based delivery systems requires the knowledge of the theoretical relation between nanocrystal size and solubility, the aim of this paper is to build up a physically-oriented thermodynamic model relating to nanocrystal dimensions with their melting temperature, enthalpy, solubility and dissolution rate. In particular, the developed model will be applied to vinpocetine, a poorly soluble drug used in the treatment of various types of cerebrovascular circulatory disorders.

Key words:
nanocrystals, drug, solubility, dissolution, thermodynamic model

1. Introduction

Regardless of the administration route, the key factor for the success and reliability of any formulation is drug bioavailability, defined as the rate and extent at which the active drug is absorbed from a pharmaceutical form and becomes available at the site of drug action.[1] Although metabolism and physiological factors highly affect drug absorption by living tissues, bioavailability is strongly dependent on drug permeability through cell membranes and on drug dissolution in physiological fluids. In particular, dissolution becomes the most important factor in terms of bioavailability for poorly water-soluble – highly permeable drugs (class II drugs according to the Amidon classification[2]). This aspect is of paramount importance if we know that, at present, about 40 % of the drugs being in the development pipelines are poorly soluble, up to 60 % of synthetized compounds are poorly soluble,[3] and 70 % of the potential drug candidates are discarded due to low bioavailability related with poor solubility in water.[4] Examples of commonly marketed drugs that are poorly soluble in water (less than 100 mg cm^{-3}) include analgesics, cardiovasculars, hormones, antivirals, immune suppressants and antibiotics.[5]

Since it is well known that solubility increases with drug nanocrystal size decrease,[5] this paper focuses on the theoretical relation existing between nanocrystal size, solubility and dissolution rate. To this end, a thermodynamic model relating to nanocrystal dimensions (radius), melting temperature/enthalpy and solubility will be presented and discussed.

2. Materials and methods

Vinpocetine ($C_{22}H_{26}N_2O_2$, molecular weight M_w = 350.45 (–)), a kind gift from Linnea SA (Riazzino-Locarno, CH, Switzerland), is a semisynthetic derivative of the Vinca minor L. alkaloid vincamine[6] used for the treatment of cognitive disorders and related symptoms such as cerebral infarction, cerebral hemorrhage residual and cerebral arteries cirrhosis.[7] This base-type drug (pKa = 7.1)[8] was chosen as a model drug because it is practically insoluble in water (1.6 μg mL^{-1} in pH = 7.4 at 37 °C).[9] Vinpocetine melting temperature ($T_{m\infty}$ = 149.6 °C), melting enthalpy ($\Delta H_{m\infty}$ = 94600 J kg^{-1}) and ΔC_p (difference in specific heat capacity at constant pressure between the liquid (C_p^l) and the solid (C_p^s), ΔC_p = 374 J kg^{-1} $°C^{-1}$) were measured by a differential scanning calorimeter (Mod. TA 4000, equipped with a measuring cell DSC 20 Mettler).

*Corresponding author: Prof. Mario Grassi;
e-mail: mariog@dicamp.univ.trieste.it; tel: 39 040 558 3435;
fax: 39 040 569823

The calibration of the instrument was performed with indium. A sample, containing about 2 mg of vinpocetine was placed in pierced aluminum pans and heated at a scanning rate of 10 °C per minute under air atmosphere. Solid vinpocetine density (ρ_s = 1268 kg m^{-3}) was measured by a helium picnometer (Quantachrome, Boynton Beach, Florida) while liquid vinpocetine density (ρ_l = 1217 kg m^{-3}) was determined as the ratio between the molecular weight M_w and the liquid vinpocetine molar volume (M_v). M_v (= 287.5 · 10^{-6} m^3 mol^{-1}) was evaluated according to the group contribution approach[10,11] implemented by the Breitkreutz software.[12]

Determination of the solid vinpocetine – vapor surface tension (γ_∞^{sv}) was performed according to the following equation of state:[13]

$$\cos(\theta_i) = 2\sqrt{\frac{\gamma_\infty^{sv}}{\gamma_i^{lv}}}\exp\left(-\beta\left(\gamma_i^{lv}-\gamma_\infty^{sv}\right)^2\right)-1 \quad (1)$$

where θ_i is the contact angle of liquid "i" on solid vinpocetine, β is a model fitting parameter and γ_i^{lv} is the liquid i – vapor surface tension. Four liquids of decreasing polarity (1-water, γ_1^{lv} = 72.8 mJ m^{-2}; 2-ethylene glycol, γ_2^{lv} = 48 mJ m^{-2}; 3-dimethyl sulfoxide, γ_3^{lv} = 44 mJ m^{-2}; 4-diiodomethane, γ_4^{lv} = 50.8 mJ m^{-2})[5] were considered. Eq. (1) fitting to experimental cos(θ_i) yielded to γ_∞^{sv} = 38.4 mJ m^{-2} and β = 1.5 · 10^{-4} (m^4 mJ^{-2}). Contact angles (water, θ_1 = 82°; ethylene glycol, θ_2 = 61°; dimethyl sulfoxide, θ_3 = 37°; diiodomethane, θ_4 = 33°) were measured by the tensiometer G10, Kruss, GmbH, Hamburg, D. Determination of the liquid vinpocetine – vapor surface tension (γ_∞^{lv}) was performed according to the Parachor method:[14]

$$\gamma_\infty^{lv} = \left(\frac{P_s}{M_v}\right)^4 = 31.2\ (\mathrm{mJ\,m^{-2}}) \quad (2)$$

The solid– liquid vinpocetine (γ_∞^{sl}) surface tension was evaluated according to the Young equation for pure substances (θ = 0):[15]

$$\gamma_\infty^{sl} = \gamma_\infty^{sv} - \gamma_\infty^{lv} = 7.2\ (\mathrm{mJ\,m^{-2}}) \quad (3)$$

The solid vinpocetine – water (γ_1^{sl}) surface tension was evaluated according to the Young equation[15] (θ_1 = 82°):

$$\gamma_1^{sl} = \gamma_\infty^{sv} - \gamma_1^{lv}\cos(\theta_1) = 27.8\ (\mathrm{mJ\,m^{-2}}) \quad (4)$$

The Tolman length δ[16] for vinpocetine (δ is equal to 1/3 of vinpocetine molecule diameter[17]) was evaluated resorting to the knowledge of liquid vinpocetine molar volume M_v and assuming a spherical shape for the vinpocetine molecule:

$$\delta = \frac{1}{3}\sqrt[3]{\frac{6M_v}{N_A\pi}} = 0.32\ (\mathrm{nm}) \quad (5)$$

where N_A is the Avogadro number.

Finally, the Crystallographic Information File (CIF) of vinpocetine was extracted from the International Union of Crystallography database.[18] Vinpocetine shows a monoclinic crystal system with the following unit cell parameters: a = 0.8907 nm, α_a = 90°, b = 0.953 nm, β_b = 106.57°, c = 0.11286 nm, γ_c = 90°, unit cell volume 0.9182 nm^3. Vinpocetine unit cell corresponds to a sphere of radius approximately equal to 0.5 nm.

3. Drug dissolution

The dissolution of a solid in a solvent is a rather complex process determined by a multiplicity of physicochemical properties of the solute and solvent.[5] Typically, for a fixed solid-solvent couple, solid solubility, liquid environment fluido-dynamic conditions, dissolution surface and solid wettability are the key factors affecting the dissolution kinetics.[5,19] In addition, for what concerns solid solubility, temperature and pH play predominant roles whilst pressure is generally less important. However, pH becomes the key parameter for the crowded class of small organic drugs behaving as weak acids or bases.[20] Indeed, as the solubility of the dissociated form can be much higher than that of the un-dissociated form, the relation between environmental pH and drug pKa being fundamental. For example, nimesulide (pKa = 6.5),[21] a weak acid nonsteroidal anti-inflammatory drug, increases its solubility by about one order of magnitude, from pH = 1.2 (37 °C: solubility ~ 10 μg mL^{-1}; nimesulide is un-dissociated) to pH = 7.5 (37 °C: ~ 100 μg mL^{-1}; nimesulide is dissociated).[22] When temperature and pH are fixed, it is well known that solubility also depends on the solid melting temperature and enthalpy[23] that, in turn, depend on solid crystals dimensions, as discussed in the next sections 4 and 5. In particular, the smaller the crystals, the lower their melting temperature/enthalpy and, consequently, the higher their solubility. Accordingly, in order to discern the effect of equilibrium (solid solubility) and kinetics (fluido-dynamic conditions, wettability, and dissolution surface) factors, let us focus on the dissolution process of a solid phase subdivided in many spherical particles, having the same diameter. In addition, we assume that particles do not aggregate during dissolution and that the initial amount of the solid phase (M_0) is so high that at equilibrium (i.e. when solid concentration reaches solubility in the liquid phase) the variation of the solid particles radius is negligible. Accordingly, for the generic solid

particle, the physical situation we are referring to is depicted in Fig. 1. Dissolution can be considered as a consecutive process driven by four energy changes ΔE_i: 1) Contact of the solvent with the solid surface (*wetting*), which implies the production of a solid–liquid interface starting from solid–vapor one ($\Delta E_1 = \Delta E_w$) 2) Breakdown of molecular bonds of the solid (*fusion*; ($\Delta E_2 = \Delta E_f$)) 3) Solid molecules transfer to the solid–liquid interface (*solvation*; ($\Delta E_3 = \Delta E_s$)) 4) Movement of the solvated molecules from the interfacial region into the bulk solution (*diffusion*; ($\Delta E_4 = \Delta E_d$)). The sum of the energies relative to the four mentioned steps represents the total energy required for solid dissolution. Obviously, the higher the dissolution energy required, the lower the dissolution kinetics. In order to connect these four energy contributes to the equilibrium and the kinetics parameters ruling solid dissolution, we need a mathematical model linking the time evolution of the solid concentration profile ($C(r)$) in the stagnant layer with the solid molecules concentration in the bulk liquid (C_b). Obviously, $C(r)$ is given by the solution of the so-called second Fick's law:

$$\frac{\partial C}{\partial t} = \nabla\left(D\nabla C\right) = \frac{1}{r^2}\frac{\partial}{\partial r}\left(Dr^2\frac{\partial C}{\partial r}\right) \tag{6}$$

where t is time, r is the radial position and D is the solid molecules diffusion coefficient in the stagnant layer (D can be considered constant in the stagnant layer thickness[5]). Assuming that a pseudo-stationary condition can be rapidly achieved in the stagnant layer (this hypothesis is supported by the numerical solution of eq. (6) assuming usual values for D ($\sim 10^{-10}$ m^2 s^{-1})[5] and stagnant layer thickness (h_{SL}) lower than 20 μm), eq. (6) becomes:

$$\frac{\partial}{\partial r}\left(Dr^2\frac{\partial C}{\partial r}\right) = 0 \tag{7}$$

The solution of eq. (7), subjected to the following initial boundary conditions:

initial:

$$C(r) = 0 \qquad R_c < r < R_s \tag{8}$$

boundary:

$$C(R_s) = C_b \tag{9}$$

$$D\left.\frac{\partial C}{\partial r}\right|_{R_c} = -k_m\left(C_s - C\left(R_c\right)\right) \tag{10}$$

leads to the solid molecule concentration profile $C(r)$ in the stagnant layer surrounding the solid particles (see details in Appendix):

$$C\left(r\right) = C_b + \frac{\left(C_s - C_b\right)R_c^2\left(k_m/k_d\right)}{h_{SL}\left(R_s + \left(k_m/k_d\right)R_c\right)}\left(\frac{R_s}{r} - 1\right) \tag{11}$$

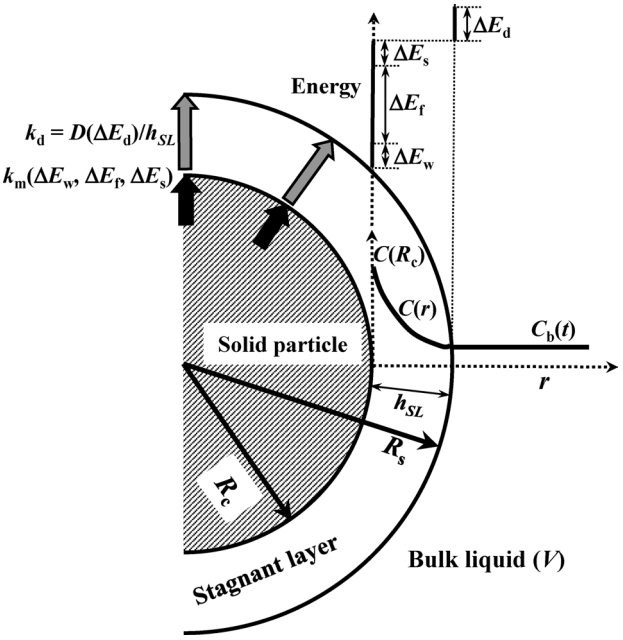

Fig. 1 – *Solid drug dissolution in a solvent liquid phase implies overcoming four energy barriers represented by solid wetting (ΔE_w), breakdown (fusion) of solid molecular bonds (ΔE_f), drug molecules solvation (ΔE_s) and drug molecules diffusion through the solvent stagnant layer to reach the bulk solvent (ΔE_d). These energies affect, in different manners, the mass transfer coefficient (k_m) at the solid/liquid interface, the dissolution constant k_d and the drug solubility $C_s(\Delta E_f)$. It is important to stress that, due to possible solid surface wetting problems, the solid molecule concentration at the solid/liquid interface ($C(R_c)$) can be lower than C_s, as shown by eq. (11).*

where R_c is the particle radius (supposed time independent; see Fig. 1), R_s is the stagnant layer radius (supposed time independent; see Fig. 1), $1/k_m$ is the solid-liquid interface mass transfer resistance while k_d (= D/h_{SL}; $h_{SL} = R_s - R_c$) is the so-called dissolution constant.[5] While eq. (8) simply states that the stagnant layer is initially drug empty, eq. (9) affirms that, in R_s, the solid molecules concentration equals the bulk one. Finally, eq. (10) affirms that solid molecules flux at the solid–liquid interface (R_c) depends on both k_m and the difference between drug solubility (C_s) and actual local drug concentration ($C(R_c)$). An inspection of eq. (11) reveals that $C(R_c)$ develops from a fraction of C_s (for $t = 0$, $C_b = 0$ and $C(R_c) = C_s\,(k_m/k_d)R_c/(R_s + (k_m/k_d)R_c)$) to C_s for a very long time. This is due to the mass transfer resistance ($1/k_m$) that accounts also for solid surface wettability problems. Indeed, when this resistance is zero, $C(R_c)$ is always equal to C_s.

In order to complete the dissolution model, it is necessary to consider the following equation:

$$V\frac{\mathrm{d}C_b}{\mathrm{d}t} = -N_p\pi R_s^2 D\left.\frac{\partial C}{\partial r}\right|_{R_s} \overset{\text{eq.(11)}}{=} \alpha\left(C_s - C_b\right)$$

$$\alpha V = \frac{3M_0}{4\rho_s R_c}\frac{k_m}{1 + \dfrac{k_m R_c}{k_d R_s}} \tag{12}$$

Eq. (12) imposes that the increase rate of the solid molecules concentration in the bulk liquid (volume V) depends on the mass flux in R_s and on the release surface ($4N_p\pi R_s^2$), being N_p the number of particles considered and ρ_s their density. Eq. (12) solution (see details in Appendix) is:

$$C_b(t) = C_s\left(1-\exp\left(-\frac{3M_0}{\rho_s R_c V}\frac{k_m}{1+\frac{k_m R_c}{k_d R_s}}t\right)\right) \quad (13)$$

Assuming, for the sake of simplicity, that the ratio R_c/R_s does not sensibly depend on R_c, eq. (13) indicates that a reduction of particles radius (R_c), being constant V and M_0, implies the improvement of the dissolution kinetics as the dissolution surface increases proportionally to $M_0/(R_c\rho_s)$. However, it will be demonstrated in the following sections 4 and 5 that R_c reduction also implies a dissolution kinetics increase due to C_s increase. It is worth noting that this last effect becomes important only for very small particles (R_c < 50 nm). On the basis of eq. (13) and Fig. 1, it is possible to argue that k_m and, thus, $1/k_m$, depend on ΔE_w, ΔE_f and ΔE_s ($k_m \to \infty$ when crystal breakdown is very fast, no wettability problems occur (solid/liquid contact angle less than ≈ 30°) and solvation is very rapid). At the same time, k_d depends on ΔE_d (the lower this energy, the higher the solid molecules mobility (D) in the stagnant layer), while C_s depends only on ΔE_f (at fixed temperature and pH) as discussed in sections 4 and 5.

4. Nanocrystal solubility dependence on melting enthalpy/temperature

The peculiar behavior of very small crystals is explained by the different characteristics of the surface and bulk phases. Indeed, due to their less confined arrangement (fewer inter-atomic bonds),[24] surface atoms/molecules are characterized by a higher energy content with respect to bulk atoms/molecules. Consequently, lattice breakdown on crystal surface would require less energy and would be favored over bulk lattice breakdown. This theoretical interpretation, supported by experimental data and molecular dynamics simulations,[25] clearly reveals the importance of surfaces as stand-alone phases. Obviously, the effect of surfaces becomes relevant (i.e., appreciable at the macroscopic level) only when the number of surface atoms/molecules is not negligible compared to that of the bulk atoms/molecules, which happens when the crystal surface/volume ratio is very high, i.e. when crystal size falls in the nanometer range.[26] The immediate consequence of the different behavior of surface atoms/molecules is that nanocrystals are characterized by a decreasing melting temperature/enthalpy as the nanocrystal radius (R_c) decreases. The thermodynamic equilibrium condition between a liquid phase (solvent) and a solid phase (drug) yields to the C_s dependence on solid crystals radius R_c, provided that the solid surface properties are properly accounted for.[26,27] Assuming that only the drug partitions between the two phases (this means that the solvent does not go inside the drug), the equilibrium condition requires that the solid drug fugacity ($\hat{f}_d^s$) and liquid phase drug fugacity ($\hat{f}_d^l$) are equal:

$$\hat{f}_d^l = \gamma_d X_d f_d^l = \hat{f}_d^s = f_d^s \quad (14)$$

where γ_d and X_d are, respectively, the drug activity coefficient and solubility (molar fraction) in the solvent, f_d^l is the drug fugacity in the reference state, while f_d^s is the drug fugacity in the solid state. Thus, X_d is given by:

$$X_d = \frac{f_d^s}{f_d^l}\frac{1}{\gamma_d} \quad (15)$$

If we assume that f_d^l is the fugacity of the pure drug in the state of undercooled liquid at system temperature (T) and pressure (P), the ratio f_d^s/f_d^l can be evaluated as the variation of the molar Gibbs free energy (Δg_{da}) between the state of undercooled liquid drug (state d) and solid (nanocrystalline) drug (state a) (see Fig. 2):

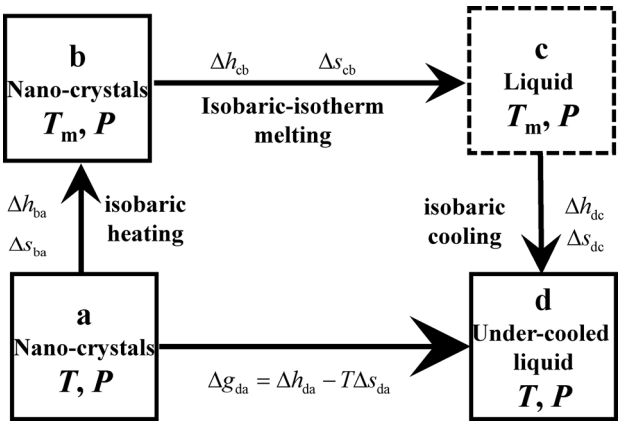

Fig. 2 – *Thermodynamic cycle used to estimate the ratio* f_d^s/f_d^l *(solid drug fugacity in the reference state "a" / drug fugacity in the state of undercooled liquid (state "d")). This ratio is linked to the Gibbs free energy variation between states "a" and "d" (*Δg_{da}*), by the relation:* $\Delta g_{da} = RT\ln\left(f_d^l/f_d^s\right)$*. g, s and h indicate, respectively, the molar Gibbs energy, entropy and enthalpy.* T_m *is the nanocrystals melting enthalpy. Adapted from ref. 26.*

$$\Delta g_{da} = RT\ln\left(f_{\mathrm{d}}^{\mathrm{l}}/f_{\mathrm{d}}^{\mathrm{s}}\right) = \Delta h_{\mathrm{da}} - T\Delta s_{\mathrm{da}} = \\ = \left(\Delta h_{\mathrm{ba}} + \Delta h_{\mathrm{cb}} + \Delta h_{\mathrm{dc}}\right) - T\left(\Delta s_{\mathrm{ba}} + \Delta s_{\mathrm{cb}} + \Delta s_{\mathrm{dc}}\right) \quad (16)$$

where R is the universal gas constant, while the enthalpy (Δh_{ba}, Δh_{cb}, Δh_{dc}) and entropy (Δs_{ba}, Δs_{cb}, Δs_{dc}) variations can be evaluated as:

$$\Delta h_{\mathrm{ba}} = \int_{T}^{T_{\mathrm{m}}} c_{\mathrm{p}}^{\mathrm{s}}\mathrm{d}T \approx c_{\mathrm{p}}^{\mathrm{s}}\left(T_{\mathrm{m}} - T\right)$$

$$\Delta s_{\mathrm{ba}} = \int_{T}^{T_{\mathrm{m}}} \frac{c_{\mathrm{p}}^{\mathrm{s}}}{T}\mathrm{d}T \approx c_{\mathrm{p}}^{\mathrm{s}}\ln\left(T_{\mathrm{m}}/T\right) \quad [\text{as } \mathrm{d}P = 0] \quad (17)$$

$$\Delta h_{\mathrm{cb}} = \Delta h_{\mathrm{m}} \qquad \Delta s_{\mathrm{cb}} = \Delta h_{\mathrm{m}}/T_{\mathrm{m}} \quad [\text{as } \Delta g_{\mathrm{m}} = \Delta h_{\mathrm{m}} - T_{\mathrm{m}}\Delta s_{\mathrm{m}} = 0\,] \quad (18)$$

$$\Delta h_{\mathrm{dc}} = \int_{T_{\mathrm{m}}}^{T} c_{\mathrm{p}}^{\mathrm{l}}\mathrm{d}T \approx c_{\mathrm{p}}^{\mathrm{l}}\left(T - T_{\mathrm{m}}\right)$$

$$\Delta s_{\mathrm{dc}} = \int_{T_{\mathrm{m}}}^{T} \frac{c_{\mathrm{p}}^{\mathrm{l}}}{T}\mathrm{d}T \approx c_{\mathrm{p}}^{\mathrm{l}}\ln\left(T/T_{\mathrm{m}}\right) \quad [\text{as } \mathrm{d}P = 0] \quad (19)$$

where T_{m} is the nanocrystal melting temperature, $c_{\mathrm{p}}^{\mathrm{s}}$ and $c_{\mathrm{p}}^{\mathrm{l}}$ are, respectively, the solid (drug) and liquid (drug) molar specific heat at constant pressure while Δg_{m}, Δh_{m} and Δs_{m} are, respectively, the molar nanocrystals melting Gibbs free energy, enthalpy and entropy. Upon rearrangement of eqs. (16)–(19), drug solubility can be expressed as a function of determinable parameters:[26,27]

$$X_{\mathrm{d}} = \frac{1}{\gamma_{\mathrm{d}}}\left(\frac{T}{T_{\mathrm{m}}}\right)^{\Delta c_{\mathrm{p}}/R} \cdot \\ \cdot \exp\left(-\left[\frac{\Delta h_{\mathrm{m}}}{RT}\left(1 - \frac{T}{T_{\mathrm{m}}}\right) + \frac{\Delta c_{\mathrm{p}}}{R}\left(1 - \frac{T_{\mathrm{m}}}{T}\right)\right]\right) \quad (20)$$

where $\mathrm{D}c_{\mathrm{p}} = c_{\mathrm{p}}^{\mathrm{l}} - c_{\mathrm{p}}^{\mathrm{s}}$.

Finally, molar solubility X_{d} can be expressed as the mass/volume solubility C_{s}:

$$C_{\mathrm{s}} = \frac{X_{\mathrm{d}}}{1 - X_{\mathrm{d}}}\frac{M_{\mathrm{d}}}{M_{\mathrm{s}}}\rho_{\mathrm{sol}} \quad (21)$$

where M_{d} and M_{s} are drug and solvent molecular weight, respectively, while ρ_{sol} is solvent density. In order to understand the effect of nanocrystal radius R_{c} decrease on X_{d} or C_{s}, the dependence of Δh_{m} and T_{m} on R_{c} has to be necessarily expressed.

5. Melting enthalpy/temperature dependence on nanocrystal radius

The physics of nanocrystals melting can be described by the three different mechanisms[28] reported in Fig. 3. According to the *Homogeneous Melting approach* (*HM*), the solid (spherical) crystal is in equilibrium with a liquid (spherical) phase having the same mass and both are embedded in the vapor phase. The *Liquid Skin Melting* theory (*LSM*) assumes the formation of a thin liquid layer over the solid core. The thickness of the liquid layer remains constant until the solid core completely melts. On the contrary, in the *Liquid Nucleation and Growth* approach (*LNG*), the liquid layer thickness increases as it approaches the melting temperature. Accordingly, the solid core melting takes place when the liquid layer thickness is no longer negligible in comparison to the solid core radius.

Fig. 3 – *Melting mechanisms: Homogeneous Melting, Liquid Skin Melting, Liquid Nucleation and Growth. R^{v} indicates the radius of the vapor phase while R^{sv}, R^{lv} and R^{sl} are, respectively, the solid-vapor, liquid-vapor and solid-liquid interface radii. Adapted from ref. 26.*

In a previously published work,[26] we theoretically demonstrated the connection existing among melting temperature/enthalpy and nanocrystals radius (R_{c}). In particular, efforts were made to properly express the infinitesimal, reversible, variation of the internal energy E (dE) referred to the closed system composed of solid drug, liquid drug and vapor drug. In that demonstration, the connection among dE and the *LSM*, *LNG*, *HM* frames (i.e. the relations existing among the solid, liquid and vapor phases; see Fig. 3) was introduced only in a late stage of the demonstration. In this work, on the contrary, we would like to follow a more physically-oriented strategy aimed to immediately consider the relations existing among the three phases according to the *LSM*, *LNG*, *HM* mechanisms. We believe that the coincidence of the final results, coming from the two approaches, strengthens the whole theoretical approach.

LSM and LNG mechanisms

The starting point is the definition of dE for the closed system (no matter or energy exchanges with

the surroundings, i.e. system volume, entropy and moles number are constant) composed of one component and 3 phases (*s* solid, *l* liquid, *v* vapor)[15] whose spatial organization is that of the *LNG* and *LSM* melting mechanisms (see Fig. 3):

$$\mathrm{d}E = \mathrm{d}E^{\mathrm{s}} + \mathrm{d}E^{\mathrm{l}} + \mathrm{d}E^{\mathrm{v}} + \mathrm{d}E^{\mathrm{sl}} + \mathrm{d}E^{\mathrm{lv}} \qquad (22)$$

where E^{s}, E^{l}, E^{v}, E^{sl}, E^{lv} represent the solid, liquid, vapor, solid/liquid and liquid/vapor phase internal energy, respectively. Assuming that a) the contribution of the first and the second curvatures to system internal energy, E, is negligible (this is strictly true for planes and spheres), and that b) thermal and chemical equilibrium is attained among the bulk and surface phases (same temperature and chemical potential in all bulk and surface phases), eq. (22) becomes:

$$\mathrm{d}E = -P^{\mathrm{v}}\mathrm{d}V^{\mathrm{v}} - P^{\mathrm{s}}\mathrm{d}V^{\mathrm{s}} - P^{\mathrm{l}}\mathrm{d}V^{\mathrm{l}} + \gamma^{\mathrm{sl}}\mathrm{d}A^{\mathrm{sl}} + \gamma^{\mathrm{lv}}\mathrm{d}A^{\mathrm{lv}} \qquad (23)$$

where P is pressure, V is volume, A is interfacial area, γ is interfacial tension while superscripts *sl* and *lv* are solid-liquid and liquid-vapor, respectively. In the light of the closed system hypothesis ($\mathrm{d}V^{\mathrm{l}} = -\mathrm{d}V^{\mathrm{v}} - \mathrm{d}V^{\mathrm{s}}$), we have:

$$\begin{aligned}\mathrm{d}E = \mathrm{d}V^{\mathrm{v}}\left(P^{\mathrm{l}} - P^{\mathrm{v}}\right) - \mathrm{d}V^{\mathrm{s}}\left(P^{\mathrm{s}} - P^{\mathrm{l}}\right) + \\ + \gamma^{\mathrm{sl}}\mathrm{d}A^{\mathrm{sl}} + \gamma^{\mathrm{lv}}\mathrm{d}A^{\mathrm{lv}}\end{aligned} \qquad (24)$$

The system equilibrium condition ($\mathrm{d}E = 0$) implies:

$$\begin{aligned}\left(P^{\mathrm{l}} - P^{\mathrm{v}}\right) &= \gamma^{\mathrm{lv}}\,\mathrm{d}A^{\mathrm{lv}}/\mathrm{d}V^{\mathrm{v}} \\ \mathrm{d}P^{\mathrm{v}} &= \mathrm{d}P^{\mathrm{l}} + \gamma^{\mathrm{lv}}\,\mathrm{d}A^{\mathrm{lv}}/\mathrm{d}V^{\mathrm{v}}\end{aligned} \qquad (25)$$

$$\begin{aligned}\left(P^{\mathrm{s}} - P^{\mathrm{l}}\right) &= \gamma^{\mathrm{sl}}\,\mathrm{d}A^{\mathrm{sl}}/\mathrm{d}V^{\mathrm{s}} \\ \mathrm{d}P^{\mathrm{s}} &= \mathrm{d}P^{\mathrm{l}} + \gamma^{\mathrm{sl}}\,\mathrm{d}A^{\mathrm{sl}}/\mathrm{d}V^{\mathrm{s}}\end{aligned} \qquad (26)$$

These relations can be inserted in the Gibbs-Duhem equation referring to the solid, liquid and vapor phases:

$$s^{\mathrm{s}}\mathrm{d}T + \mathrm{d}\mu_1 - v^{\mathrm{s}}\mathrm{d}P^{s} = 0 \qquad \text{solid} \qquad (27)$$

$$s^{\mathrm{l}}\mathrm{d}T + \mathrm{d}\mu_1 - v^{\mathrm{l}}\mathrm{d}P^{l} = 0 \qquad \text{liquid} \qquad (28)$$

$$s^{\mathrm{v}}\mathrm{d}T + \mathrm{d}\mu_1 - v^{\mathrm{v}}\mathrm{d}P^{v} = 0 \qquad \text{vapor} \qquad (29)$$

where s^{s}, s^{l} and s^{v} indicate the molar entropy of the solid, liquid and vapor phases, respectively, μ_1 is the chemical potential (equal for all three phases in hypothesis (b)), v^{s}, v^{l} and v^{v} are, respectively, the molar volume of the solid, liquid and vapor phases, and T is temperature. Subtracting eq. (28) from eq. (27) and eq. (29) from eq. (28) leads to:

$$\left(s^{\mathrm{s}} - s^{\mathrm{l}}\right)\mathrm{d}T - v^{\mathrm{s}}\mathrm{d}P^{s} + v^{\mathrm{l}}\mathrm{d}P^{l} = 0 \qquad (30)$$

$$\left(s^{\mathrm{l}} - s^{\mathrm{v}}\right)\mathrm{d}T - v^{\mathrm{l}}\mathrm{d}P^{l} + v^{\mathrm{v}}\mathrm{d}P^{v} = 0 \qquad (31)$$

Inserting in eqs. (30)–(31) the expressions of $\mathrm{d}P^{\mathrm{v}}$ and $\mathrm{d}P^{\mathrm{s}}$ coming from eqs. (25) and (26) leads to:

$$\mathrm{d}P^{\mathrm{l}} = \frac{s^{\mathrm{s}} - s^{\mathrm{l}}}{v^{\mathrm{s}} - v^{\mathrm{l}}}\mathrm{d}T - \frac{v^{\mathrm{s}}}{v^{\mathrm{s}} - v^{\mathrm{l}}}\mathrm{d}\left(\gamma^{\mathrm{sl}}\,\mathrm{d}A^{\mathrm{sl}}/\mathrm{d}V^{\mathrm{s}}\right) \qquad (32)$$

$$\mathrm{d}P^{\mathrm{l}} = \frac{s^{\mathrm{l}} - s^{\mathrm{v}}}{v^{\mathrm{l}} - v^{\mathrm{v}}}\mathrm{d}T + \frac{v^{\mathrm{v}}}{v^{\mathrm{l}} - v^{\mathrm{v}}}\mathrm{d}\left(\gamma^{\mathrm{lv}}\,\mathrm{d}A^{\mathrm{lv}}/\mathrm{d}V^{\mathrm{v}}\right) \qquad (33)$$

Equating eqs. (32) to (33), we have:

$$\begin{aligned}\left(\frac{s^{\mathrm{s}} - s^{\mathrm{l}}}{v^{\mathrm{s}} - v^{\mathrm{l}}} - \frac{s^{\mathrm{l}} - s^{\mathrm{v}}}{v^{\mathrm{l}} - v^{\mathrm{v}}}\right)\mathrm{d}T = \frac{v^{\mathrm{s}}}{v^{\mathrm{s}} - v^{\mathrm{l}}}\mathrm{d}\left(\gamma^{\mathrm{sl}}\,\mathrm{d}A^{\mathrm{sl}}/\mathrm{d}V^{\mathrm{s}}\right) + \\ + \frac{v^{\mathrm{v}}}{v^{\mathrm{l}} - v^{\mathrm{v}}}\mathrm{d}\left(\gamma^{\mathrm{lv}}\,\mathrm{d}A^{\mathrm{lv}}/\mathrm{d}V^{\mathrm{v}}\right)\end{aligned} \qquad (34)$$

Remembering that $v^{\mathrm{v}} >> v^{\mathrm{l}} \approx v^{\mathrm{s}}$, it follows $\left|\frac{s^{\mathrm{l}} - s^{\mathrm{v}}}{v^{\mathrm{l}} - v^{\mathrm{v}}}\right| << \left|\frac{s^{\mathrm{s}} - s^{\mathrm{l}}}{v^{\mathrm{s}} - v^{\mathrm{l}}}\right|$ and $v^{\mathrm{v}}/(v^{\mathrm{l}} - v^{\mathrm{v}}) \approx -1$. Thus, eq. (34) becomes:

$$\begin{aligned}\Delta s_{\mathrm{m}}\mathrm{d}T = \left(v^{\mathrm{s}} - v^{\mathrm{l}}\right)\mathrm{d}\left(\gamma^{\mathrm{lv}}\,\mathrm{d}A^{\mathrm{lv}}/\mathrm{d}V^{\mathrm{v}}\right) - \\ - v^{\mathrm{s}}\mathrm{d}\left(\gamma^{\mathrm{sl}}\,\mathrm{d}A^{\mathrm{sl}}/\mathrm{d}V^{\mathrm{s}}\right)\end{aligned} \qquad (35)$$

where Δs_{m} is the molar melting entropy ($s^{\mathrm{l}} - s^{\mathrm{s}}$). In order to make eq. (35) operative, it is necessary to evaluate the two differential terms involving areas, volumes and surface tensions. In particular, for spherical crystals, we have:

$$\begin{aligned}A^{\mathrm{sl}} &= 4\pi R_{\mathrm{sl}}^2 \qquad \mathrm{d}A^{\mathrm{sl}} = 8\pi R_{\mathrm{sl}} dR_{\mathrm{sl}} \\ V^{\mathrm{s}} &= (4/3)\pi R_{\mathrm{sl}}^3 \qquad dV^{\mathrm{s}} = 4\pi R_{\mathrm{sl}}^2 \mathrm{d}R_{\mathrm{sl}}\end{aligned} \qquad (36)$$

$$\begin{aligned}A^{\mathrm{lv}} &= 4\pi R_{\mathrm{lv}}^2 \qquad \mathrm{d}A^{\mathrm{lv}} = 8\pi R_{\mathrm{lv}} dR_{\mathrm{lv}} \\ V^{\mathrm{v}} &= (4\pi/3)\left(R_{\mathrm{v}}^3 - R_{\mathrm{sl}}^3\right) \qquad dV^{\mathrm{v}} = -4\pi R_{\mathrm{lv}}^2 \mathrm{d}R_{\mathrm{lv}}\end{aligned} \qquad (37)$$

$$\mathrm{d}A^{\mathrm{sl}}/\mathrm{d}V^{\mathrm{s}} = 2/R_{\mathrm{sl}} \qquad \mathrm{d}A^{\mathrm{lv}}/\mathrm{d}V^{\mathrm{v}} = -2/R_{\mathrm{lv}} \qquad (38)$$

where R_{sl} and R_{lv} represent the curvature radius proper to the solid-liquid and liquid-vapor interface, respectively (see Fig. 3). In addition, the surface tension γ dependence on the interface curvature radius, as suggested by Tolman,[16] is as follows:

$$\frac{\gamma}{\gamma_\infty} = \left(1 + \frac{2\delta}{R_{\mathrm{c}}}\right)^{-1} \qquad (39)$$

where γ_∞ and γ are, respectively, the surface tension competing to a flat surface (infinite curvature radius) and a surface of curvature radius R_c, while δ is the Tolman length whose order of magnitude should correspond to the effective molecular diameter m_d and it is usually assumed[17] to be $m_d/3$. On the basis of eqs. (36)–(39), eq. (35) becomes:

$$\frac{\Delta h_m}{T}\mathrm{d}T = 2\left(v^l - v^s\right)\mathrm{d}\left(\frac{\gamma_\infty^{lv}}{R_{lv}+2\delta}\right) - 2v^s\mathrm{d}\left(\frac{\gamma_\infty^{sl}}{R_{sl}+2\delta}\right) \quad (40)$$

where Δh_m is the molar melting enthalpy. The integration of eq. (40) between the melting temperature of the infinitely large crystal ($T_{m\infty}$, $R_{lv}\to\infty$, $R_{sl}\to\infty$) and the melting temperature (T_m) of the crystal of radius R_{sl}, leads to:

$$\int_{T_{m\infty}}^{T_m}\frac{\Delta h_m}{T}\mathrm{d}T = \frac{2\gamma_\infty^{lv}}{R_{lv}+2\delta}\left(v^l - v^s\right) - 2v^s\frac{\gamma_\infty^{sl}}{R_{sl}+2\delta} \quad (41)$$

or, expressing the enthalpy per unit mass instead of per mole:

$$\int_{T_{m\infty}}^{T_m}\frac{\Delta H_m}{T}\mathrm{d}T = \frac{2\gamma_\infty^{lv}}{R_{lv}+2\delta}\left(\frac{1}{\rho_l}-\frac{1}{\rho_s}\right) - \frac{2\gamma_\infty^{sl}}{\rho_s\left(R_{sl}+2\delta\right)} \quad (42)$$

where ρ_l and ρ_s are, respectively the density of the liquid and solid phases. Establishing a relation between R_{lv} and R_{sl} is now essential. To this end, a generalized version of the strategy adopted by Coceani[27] can be undertaken. This approach relies upon the fact that, very often, drug crystals' melting occurs in the presence of a drug amorphous solid that becomes liquid before the melting temperature. Indeed, as the glass transition temperature of the amorphous drug is lower than the crystals' melting temperature (whatever R_{sl}), the amorphous drug will be liquid before the nanocrystals melting. Thus, at melting point, the nanocrystals mass fraction, X_{nc}, can be evaluated as:

$$X_{nc} = \frac{(4/3)\pi R_{sl}^3\rho_s}{(4/3)\pi R_{sl}^3\rho_s + (4/3)\pi\rho_l\left(R_{lv}^3 - R_{sl}^3\right)} = \frac{R_{sl}^3\rho_s}{R_{sl}^3\rho_s + \rho_l\left(R_{lv}^3 - R_{sl}^3\right)} \quad (43)$$

Consequently, we have:

$$R_{lv} = R_c\sqrt[3]{\frac{\rho_s}{\rho_l}\left(\frac{1-X_{nc}}{X_{nc}}\right)+1} \qquad R_c = R_{sl} \quad (44)$$

It is easy to verify that the *LSM* condition occurs for $X_{nc}\approx 1$ (the amorphous, liquid phase is virtually absent; $R_{lv}\approx R_c$), while *LNG* condition takes place for $X_{nc}\approx 0$ (nanocrystal melting occurs in a virtually infinite liquid phase, $R_{lv}\approx\infty$). For $0 < X_{nc} < 1$, we can account for what usually happens during the melting of organic drug crystals embedded in a polymeric stabilizing carrier.[27] When X_{nc} is unknown, its determination implies an iterative procedure based on the knowledge of the differential scanning calorimetry trace referring to the melting of the amorphous/crystal drug.[26,27]

It is interesting to note that the results of the approach presented in this paper lead to what was previously demonstrated following a different path.[26]

HM mechanism

In the case of the homogeneous melting, the expression of the infinitesimal, reversible, variation of the internal energy E reads:

$$\mathrm{d}E = -P^v\mathrm{d}V^v - P^s\mathrm{d}V^s - P^l\mathrm{d}V^l + \gamma^{sv}\mathrm{d}A^{sv} + \gamma^{lv}\mathrm{d}A^{lv} \quad (45)$$

It is worth noting that eq. (45) differs from eq. (23) in that the term $\gamma^{sl}\mathrm{d}A^{sl}$ is substituted by the term $\gamma^{sv}\mathrm{d}A^{sv}$. Indeed, in the *HM* case, the solid/liquid interface no longer exists (see Fig. 3), while it is replaced by the solid/vapor interface. Starting from eq. (45) and following a procedure analogue to that shown for the *LSM* and *LNG* approaches, we obtain:

$$\int_{T_{m\infty}}^{T_m}\frac{\Delta H_m}{T}\mathrm{d}T = \frac{2\gamma_\infty^{lv}}{\rho_l\left(R_{lv}+2\delta\right)} - \frac{2\gamma_\infty^{sv}}{\rho_s\left(R_{sl}+2\delta\right)} \quad (46)$$

Remembering that in the *HM* case the solid and liquid phases are characterized by the same mass, the relation between R_{lv} and R_{sl} (= R_c) is:

$$(4/3)\pi R_{sl}^3\rho_s = (4/3)\pi R_{lv}^3\rho_l \quad ==>$$
$$R_{lv} = R_c\left(\rho_s/\rho_l\right)^{1/3} \qquad R_c = R_{sl} \quad (47)$$

6. Results

In order to integrate eq. (42) and (46), it is necessary to know the ΔH_m dependence on R_c and T_m. Therefore, the thermodynamic relation used by Zhang and co-workers,[29] holding regardless of nanocrystal nature (organic or inorganic) and characterized by easily determinable parameters, seems appropriate:

$$\Delta H_m = \Delta H_{m\infty} - \frac{3}{R_c+2\delta}\left(\frac{\gamma_\infty^{sv}}{\rho_s} - \frac{\gamma_\infty^{lv}}{\rho_l}\right) - \int_{T_m}^{T_{m\infty}}\Delta C_p\mathrm{d}T \quad (48)$$

where $\Delta H_{m\infty}$ is the specific melting enthalpy (J Kg^{-1}) referred to the infinite radius drug crystal, ΔC_p (J kg^{-1} K^{-1}) is the difference between the liquid and solid drug specific heat capacity at constant pressure. As ΔC_p is almost temperature invariant, the integral in eq. (48) can be approximated by ΔC_p

($T_{m\infty} - T_m$). Figs. 4A and 4B indicate, respectively, the reduction of vinpocetine melting temperature (T_m) and melting enthalpy (ΔH_m) with crystal radius (R_c) according to eq. (42) in the case of liquid skin melting (X_{nc} = 1), liquid nucleation and growth ($X_{nc} \approx 0$) mechanisms. It can be seen that, for both mechanisms, an appreciable effect of R_c reduction takes place for $R_c < 50$ nm, while T_m and ΔH_m undergo a considerable reduction for $R_c < 10$ nm. On the contrary, the effect of X_{nc} seems limited, and this is mainly due to the fact that vinpocetine density does not significantly change from the solid to the liquid state (see eq. (42)). Interestingly, we found similar results using other poorly water soluble small organic drugs, i.e., nifedipine, griseofulvin[26] and nimesulide.[27] In the case of griseofulvin and nifedipine, model predictions were substantially confirmed by means of the *X* rays evaluation of nanocrystal dimensions.[26]

Fig. 5A shows, according to eq. (20), the increase of vinpocetine nanocrystal solubility (C_s) with R_c reduction for two different X_{nc} values (1, LNG; ≈ 0, LNG). Also in this case, an appreciable

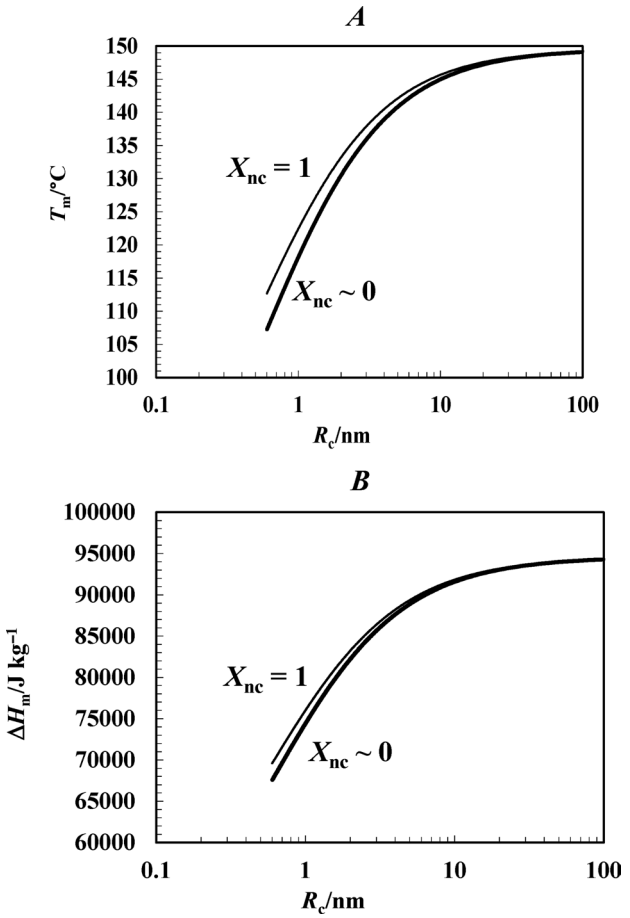

Fig. 4 – ***A)*** *Reduction of melting temperature T_m with crystal radius R_c in the case of Vinpocetine.* ***B)*** *Reduction of the melting enthalpy ΔH_m with crystal radius R_c in the case of Vinpocetine. X_{nc} is the nanocrystal mass fraction. Prediction according to eq. (42).*

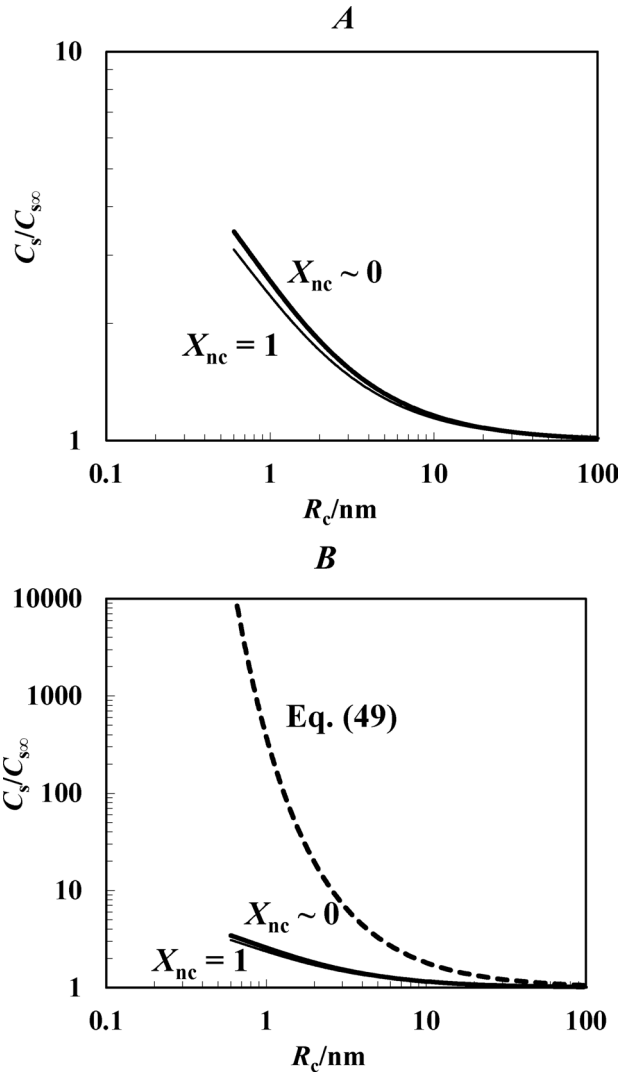

Fig. 5 – ***A)*** *Increase of vinpocetine solubility with nanocrystals radius R_c decrease according to eq. (20) and the T_m and ΔH_m trend shown in Fig. 4A, B. C_s is the solubility of the vinpocetine nanocrystal of radius R_c, while $C_{s\infty}$ is the solubility of an infinitely large vinpocetine crystal. X_{nc} is the nanocrystal mass fraction (simulations referred to 37 °C).* ***B)*** *Increase of vinpocetine solubility according to our approach (eq. (20); solid lines) and the Ostwald-Freundlich approach (eq. (49); dashed line) (simulations referred to 37 °C).*

effect takes place for $R_c < 50$ nm and the effect exerted by X_{nc} is not so relevant. For the smallest nanocrystals, C_s is about 3 times that of the infinitely large vinpocetine crystals ($C_{s\infty}$).

While model verification can be conducted, in its thermal part, e.g. with *X* ray analysis,[26] the proof of the solubility enhancement is much more difficult due to the experimental difficulty of measuring the solubility of drug nanocrystals and amorphous drugs.[30–33] Some useful considerations can be drawn by making a comparison between our model and the well-known Ostwald-Freundlich model:[34]

$$\frac{C_s}{C_{s\infty}} = \exp\left(\frac{2\gamma_1^{sl} M_{vs}}{RT}\frac{1}{R_c}\right) \qquad (49)$$

Assuming $T = 37$ °C, $M_{vs} = (= 276 \cdot 10^{-6}$ m^3 mol$^{-1})$ and the γ_1^{sl} value evaluated in section 2 (Materials and Methods), eq. (49) prediction is shown in Fig. 5B (dashed line) jointly with the predictions of our approach (solid thin and thick lines). It can be noticed that for small crystals eq. (49) leads to an unreasonable solubility increase keeping in mind that, in general, the solubility increase of amorphous drugs (not too dissimilar from vinpocetine) have been theoretically estimated in the range (7 – 100).[35] On the contrary, the prediction of our model seems more reasonable. Nevertheless, we recognize that the difficulty connected to the experimental measurement of nanocrystals solubility leaves this question still open.

7. Conclusions

In this paper, we demonstrated the theoretical correctness of our previous approach aimed at the evaluation of melting temperature/enthalpy depression with decreasing nanocrystals radius. Indeed, by means of a more physically oriented approach, we confirmed the theoretical results of our previous work. In addition, considering these results in the frame of drug dissolution, we proved that nanocrystals can play a very important role in the pharmaceutical field as they can enhance the bioavailability of poorly soluble – highly permeable drugs. Indeed, the concomitant decrease in melting temperature and enthalpy has a double beneficial effect on drug dissolution and, ultimately, on drug bioavailability. On the one hand, melting enthalpy reduction ($\Delta H_m = \Delta E_f$ at constant temperature and pressure, see Fig. 1) improves the dissolution process by reducing one of the most important energy-related steps involved in drug dissolution (i.e. breakdown of the crystalline network (step 2 in Fig. 1), connected to the mass transfer resistance $1/k_m$). On the other hand, it increases drug solubility (see eq. (20) and Fig. 5A). As a result, the dissolution rate can be increased considerably.

Interestingly, despite the mathematical (not physical) complexity connected to the theoretical study of the relation existing between nanocrystals size and solubility, the preparation of drug nanocrystals is no longer problematic since many reliable technologies are available nowadays.[36,37] This is of particular interest if we know that, until now, about 70 % of the potential drug candidates are discarded due to low bioavailability related with poor solubility in water.[4] Obviously, the problem of bioavailability enhancement of poorly soluble drugs also requires the estimation of drug solubility in the drug amorphous state that can be considered as a nanocrystal of vanishing dimensions. In this respect, the work of Bogner and co-workers[35] is a very interesting theoretical contribution.

APPENDIX

The solution of eq. (7)

$$\frac{\partial}{\partial R}\left(DR^2\frac{\partial C}{\partial R}\right)=0 \tag{7}$$

implies a double integration in space:

first: $$R^2\frac{\partial C}{\partial R}=A_1: \tag{A1}$$

second: $$\frac{\partial C}{\partial R}=\frac{A_1}{R^2} \;\Rightarrow\; C(R)=A_2-\frac{A_1}{R} \tag{A2}$$

The integration constants A_1 and A_2 can be evaluated by means of the boundary conditions expressed by eqs. (9) and (10):

$$C(R_s) = C_b \tag{9}$$

$$D\frac{\partial C}{\partial R}\bigg|_{R_c} = -k_m\left(C_s - C\left(R_c\right)\right) = \tag{10}$$

From eqs. (9) and (10), we have:

$$C\left(R_s\right) = C_b = A_2 - A_1/R_c \tag{A3}$$

$$D\frac{\partial C}{\partial R}\bigg|_{R_c} = A_1/R_c^2 = -k_m\left(C_s - A_2 + A_1/R_c\right) \tag{A4}$$

The solution of the linear system represented by eqs. (A3) and (A4) leads to the determination of the integration constants A_1 and A_2:

$$A_1 = \left(C_b - C_s\right)\frac{R_c^2\left(k_m/k_d\right)R_s}{h_{SL}\left(R_s + \left(k_m/k_d\right)R_c\right)}$$

$$A_2 = C_b + \left(C_b - C_s\right)\frac{R_c^2\left(k_m/k_d\right)}{h_{SL}\left(R_s + \left(k_m/k_d\right)R_c\right)} \tag{A5}$$

Inserting these expressions for A_1 and A_2 into eq. (A2), leads to eq. (11).

Starting from eq. (11), it is possible to solve eq. (12) since we now have an analytical expression for the spatial concentration derivative:

$$\frac{\partial C}{\partial R}\bigg|_{R_s} = \left(C_s - C_b\right)\frac{R_c^2\left(k_m/k_d\right)R_s}{h_{SL}\left(R_s + \left(k_m/k_d\right)R_c\right)}\left(-\frac{1}{R_s^2}\right) \tag{A6}$$

Substitution of eq. (A6) into eq. (12) leads to:

$$V\frac{\mathrm{d}C_b}{\mathrm{d}t} = -N_p 4\pi R_s^2 D\left(C_s - C_b\right)\cdot \cdot\frac{R_c^2\left(k_m/k_d\right)R_s}{h_{SL}\left(R_s + \left(k_m/k_d\right)R_c\right)}\left(-\frac{1}{R_s^2}\right) \tag{A7}$$

Remembering that the number of particles is given by $N_p = M_0/((4/3)\pi\rho R_c^3)$ and that $k_d = D/h_{SL}$, eq. (A7) can be rearranged to give:

$$\frac{dC_b}{dt} = \left(C_s - C_b\right)\frac{3M_0}{\rho R_c V}\frac{k_m}{\left(1+\left(k_m/k_d\right)\left(R_c/R_s\right)\right)} \quad \text{(A8)}$$

This first order differential equation can be solved by means of standard techniques to give eq. (13).

List of symbols

a – vinpocetine unit cell side, m
A^{lv} – liquid drug – vapor drug interface area, m^2
A^{sl} – solid drug – liquid drug interface area, m^2
A^{sv} – solid drug – vapor drug interface area, m^2
b – vinpocetine unit cell side, m
c – vinpocetine unit cell side, m
$C(r)$ – drug concentration profile in the stagnant layer, kg m^{-3}
C_b – drug concentration in the bulk liquid, kg m^{-3}
C_s – nanocrystals drug solubility in the bulk liquid, kg m^{-3}
$C_{s\infty}$ – infinitely wide crystals drug solubility in the bulk liquid, kg m^{-3}
C_p^l – liquid drug specific heat capacity at constant pressure, J kg^{-1} °C^{-1}
c_p^l – molar liquid drug heat capacity at constant pressure, J mol^{-1} °C^{-1}
C_p^s – solid drug specific heat capacity at constant pressure, J kg^{-1} °C^{-1}
c_p^s – molar solid drug heat capacity at constant pressure, J mol^{-1} °C^{-1}
D – drug diffusion coefficient in the liquid stagnant layer, m^2 s^{-1}
E – system internal energy, J
E^s – solid phase internal energy, J
E^l – liquid phase internal energy, J
E^v – vapor phase internal energy, J
E^{sl} – solid/liquid phase internal energy, J
E^{lv} – liquid/vapor phase internal energy, J
$\hat{f}_d^s$ – drug fugacity in the solid state, Pa
f_d^s – pure solid drug fugacity, Pa
$\hat{f}_d^l$ – drug fugacity in the liquid state, Pa
f_d^l – drug fugacity in the reference state, Pa
k_d – dissolution constant, m s^{-1}
h_{SL} – stagnant layer thickness, m
k_m – solid drug-liquid mass transfer coefficient, m s^{-1}
M_d – drug molecular weight, –
m_d – drug molecular diameter, m
M_v – liquid vinpocetine molar volume, m^3 mol^{-1}
M_{vs} – solid vinpocetine molar volume, m^3 mol^{-1}
M_s – solvent molecular weight, –
M_w – drug molecular weight, –
M_0 – initial solid drug amount considered in dissolution, kg
N_A – Avogadro number, –
N_p – numbers of solid spherical crystals involved in the dissolution process, –
P – pressure, Pa
P^l – liquid phase pressure, Pa
P^s – solid phase pressure, Pa
P^v – vapor phase pressure, Pa
P_s – Parachor, J$^{0.25}$ m$^{2.5}$/mol^{-1}
r – radial position, m
R – universal gas constant, J mol^{-1} K^{-1}
R_c – crystal radius, m
R_s – stagnant layer radius, m
R^{lv}, R_{lv} – liquid-vapor interface radius, m
R^{sl}, R_{sl} – solid-liquid interface radius, m
R^{sv}, R_{sv} – solid-vapor interface radius, m
R^v – vapor phase radius, m
s^l – molar liquid drug entropy, J mol^{-1} K^{-1}
s^s – molar solid drug entropy, J mol^{-1} K^{-1}
s^v – molar vapor drug entropy, J mol^{-1} K^{-1}
t – time, s
T – temperature, K
$T_{m\infty}$ – melting temperature of an infinitely wide drug crystal, K
V – bulk liquid volume, m^3
V^l – liquid phase volume, m^3
V^s – solid phase volume, m^3
V^v – vapor phase volume, m^3
X_d – drug molar fraction solubility, –
X_{nc} – nanocrystal mass fraction, -

Greek letters

α – eq. (12) parameter, s^{-1}
α_a – angle between directions *a* and *b,* degrees
β – model fitting parameter (eq. (1))
β_b – angle between directions *a* and *c*, degrees
δ – Tolman length, m
ΔC_p – difference between the liquid and the solid drug specific heat capacity at constant pressure, J kg^{-1} °C^{-1}
$\Delta E_1 = \Delta E_w$ – energy variation related to solid drug wetting, J
$\Delta E_2 = \Delta E_f$ – energy variation related to the breakdown of molecular bonds of the solid, J
$\Delta E_3 = \Delta E_s$ – energy variation related solid molecules solvation, J
$\Delta E_4 = \Delta E_d$ – energy variation related to the movement of the solvated molecules from the interfacial region (solid drug-liquid) into the bulk liquid solution, J

Δg_{da} – molar Gibbs energy variation from state "d" (under-cooled liquid drug at T and P) and state "a" (drug nanocrystals at T and P), J mol^{-1}

Δg_{m} – melting molar Gibb energy, J mol^{-1}

Δh_{da} – molar enthalpy variation between state "d" (under-cooled liquid drug at T and P) and state "a" (drug nanocrystals at T and P), J mol^{-1}

Δh_{ba} – molar enthalpy variation between state "b" (drug nanocrystals at T_m and P) and state "a" (drug nanocrystals at T and P), J mol^{-1}

Δh_{cb} – molar enthalpy variation between state "c" (liquid drug at T_m and P) and state "b" (drug nanocrystals at T_m and P), J mol^{-1}

Δh_{dc} – molar enthalpy variation from state "d" (under-cooled liquid drug at T and P) to state "c" (liquid drug at T_m and P), J mol^{-1}

Δh_{m} – molar melting enthalpy of nanocrystals, J mol^{-1}

$\Delta H_{m\infty}$ – specific melting enthalpy of infinitely wide crystals, J kg^{-1}

ΔH_{m} – specific melting enthalpy of nanocrystals, J kg^{-1}

Δs_{m} – nanocrystals melting molar entropy, J mol^{-1}

Δs_{da} – molar entropy variation between state "d" (under-cooled liquid drug at T and P) and state "a" (drug nanocrystals at T and P), J mol^{-1}

Δs_{ba} – molar entropy variation between state "b" (drug nanocrystals at T_m and P) and state "a" (drug nanocrystals at T and P), J mol^{-1}

Δs_{cb} – molar entropy variation between state "c" (liquid drug at T_m and P) and state "b" (drug nanocrystals at T_m and P), J mol^{-1}

Δs_{dc} – molar entropy variation from state "d" (under-cooled liquid drug at T and P) to state "c" (liquid drug at T_m and P), J mol^{-1}

γ_c – angle between directions b and c, degrees

γ_d – drug activity coefficient, -

γ_i^{lv} – liquid "i" – vapor surface tension (flat surface), J m^{-2}

γ^{lv} – liquid drug – vapor drug surface tension, J m^{-2}

γ_i^{sl} – solid drug – liquid "i" surface tension (flat surface), J m^{-2}

γ^{sl} – solid drug – liquid drug surface tension, J m^{-2}

γ_∞^{lv} – liquid vinpocetine – vapor surface tension (flat surface), J m^{-2}

γ^{sv} – solid drug – vapor drug surface tension, J m^{-2}

γ_∞^{sv} – solid drug – vapor surface tension (flat surface), J m^{-2}

γ_∞^{sl} – solid drug – liquid drug surface tension (flat surface), J m^{-2}

μ_1 – chemical potential of species "1", J mol^{-1}

v^l – liquid drug molar volume, m^3 mol^{-1}

v^s – solid drug molar volume, m^3 mol^{-1}

v^v – vapor drug molar volume, m^3 mol^{-1}

ρ_l – liquid drug density, kg m^{-3}

ρ_s – solid drug density, kg m^{-3}

ρ_{sol} – solvent density, kg m^{-3}

θ_i – contact angle of liquid "i" on solid drug, degrees

References

1. Medicinal Products for Human Use: Guidelines, Pharmacos 4, Eudralex Collection, 2005, p. 234 (http://ec.europa.eu/health/documents/eudralex/).
2. *Amidon, G. L., Lennernäs, H., Shah, V. P., Crison, J. R.*, Pharm. Res. **12** (1995) 413. http://dx.doi.org/10.1023/A:1016212804288
3. *Lipinski, C.*, Am. Pharm. Rev. **5** (2002) 82.
4. *Cooper, E. R.*, J. Control. Rel. **141** (2010) 300. http://dx.doi.org/10.1016/j.jconrel.2009.10.006
5. *Grassi, M., Grassi, G., Lapasin, R., Colombo, I.*, Understanding drug release and absorption mechanisms: a physical and mathematical approach, 2007, CRC Press, Boca Raton (FL, USA).
6. *Lorincz. C., Szasz, K., Kisfaludym, L.,* Arzneim-Forsch Drug. Res. **26** (1976) 1907.
7. *Csanda, E., Harcos, P., Bacsy, Z., Berghammer, R., Kenez, J.,* 1988. Drug. Dev. Res. **14** (1988) 185. http://dx.doi.org/10.1002/ddr.430140304
8. *Weinshaar, R. E, Bristol, J. A.*, In: Comprehensive medicinal chemistry; Hansch, C., (Ed.) Vol. II, Pergamon Press, Oxford, UK, 1990, pp 501–514.
9. *Hasa, D., Voinovich, D., Perissutti, B., Bonifacio, A., Grassi, M., Franceschinis, E., Dall'Acqua, S., Speh, M., Plavec, J., Invernizzi, S. J.,* Pharm. Sci. **100** (2011) 915. http://dx.doi.org/10.1002/jps.22331
10. *Fedors, R. F.,* Polymer Engin. Sci. **14** (1974) 147. http://dx.doi.org/10.1002/pen.760140211
11. *Van Krevelen, D. W., Hoftyzer, P. J.,* Properties of polymers. Their estimation and correlation with chemical structures. 1976. Elsevier, Amsterdam.
12. *Breitkreutz, J.,* Pharm. Res. **15** (1998) 1370. http://dx.doi.org/10.1023/A:1011941319327
13. *Kwok, D. Y., Neumann, A. W.*, Advances in Colloid and Interface Science **81** (1999) 167. http://dx.doi.org/10.1016/S0001-8686(98)00087-6
14. *Van Krevelen, D. W.,* Properties of Polymers. Their correlation with chemical structure; Their numerical estimation and prediction from additive group contribution. 3rd edition, 1990, Elsevier, Amsterdam.
15. *Adamson A. W., Gast A. P.*, Physical Chemistry of Surfaces. 1997. Wiley-Interscience, New York.
16. *Tolman, R. C.,* J. Chem. Phys. **17** (1949) 333. http://dx.doi.org/10.1063/1.1747247
17. *Rowlinson, J. S., Windom, B.*, Molecular theory of capillarity. 1982. Clarendon Press, Oxford.
18. *Kawashima, Y., Ikemoto, T., Horiguchi, A., Hayashi, M., Matsumoto, K., Kawarasaki, K., Yamazaki, R., Okuyama, S., Hatayama K.,* J. Med. Chem. **36** (1993) 815. http://dx.doi.org/10.1021/jm00059a004
19. *Levich, V. G.*, Physicochemical Hydrodynamics, Englewood Cliffs, N.J., Prentice-Hall, 1962.
20. *Avdeef, A.,* Absorption and drug development: solubility, permeability and charge state. 2012. 2nd ed. Wiley, Hoboken. http://dx.doi.org/10.1002/9781118286067
21. *Ravichandiran, V., Devarajan, V., Masilamani, K.*, Der Pharmacia Lettre **3** (2011) 183.
22. *Grassi, M., Coceani, N., Magarotto, L.*, Int. J. Pharm. **239** (2002) 157. http://dx.doi.org/10.1016/S0378–5173(02)00101–1
23. *Poling, B. E., Prausnitz, J. M., O'Connell, J. P.,* The Properties of Gases and Liquids, 5th ed. 2004. McGraw-Hill, New York.
24. *Lubashenko, V. V.,* J. Nanopart. Res. **12** (2010) 1837. http://dx.doi.org/10.1038/nmat2132

25. *Huang, W. J., Sun, R., Tao, J., Menard, L. D., Nuzzo, R. G., Zuo, J. M.,* Nature Materials **7** (2008) 308. http://dx.doi.org/10.1038/nmat2132
26. *Hasa, D., Voinovich, D., Perissutti, B., Grassi, G., Fiorentino, S., Farra, R., Abrami, M., Colombo, I., Grassi, M.*, Eur. J. Pharm. **50** (2013) 17. http://dx.doi.org/10.1016/j.ejps.2013.03.018
27. *Coceani, N., Magarotto, L., Ceschia, D., Colombo, I., Grassi, M.,* Chem. Eng. Sci. **71** (2012) 345. http://dx.doi.org/10.1016/j.ces.2011.12.036
28. *Nanda, K. K.*, Pramana Journal of Physics **72** (2009) 617.
29. *Zhang, M., Efremov, M. Y., Schiettekatte, F., Olson, E. A., Kwan, A. T., Lai, S. L., Wisleder, T., Greene, J. E., Allen, L. H.*, Physical Review *B* **62** (2000) 10548. http://dx.doi.org/10.1103/PhysRevB.62.10548
30. *Mosharraf, M., Nystrom, C.*, Drug Dev. Ind. Pharm. **29** (2003) 603. http://dx.doi.org/10.1081/DDC-120021310
31. *Madras, G., McCoy, B. J.*, Crys. Gro. Des., **3** (2003) 981. http://dx.doi.org/10.1021/cg034117l
32. *Murdande, S. B., Pikal, M. J., Shanker, R. M., Bogner, R. H.*, Pharm. Res. **27** (2010) 2704. http://dx.doi.org/10.1007/s11095–010–0269–5
33. *Murdande, S. B., Pikal, M. J., Shanker, R. M., Bogner, R. H.*, J Pharm. Sci. **100** (2011) 4349. http://dx.doi.org/10.1002/jps.22643
34. *Ostwald, W. Z.,* Phys. Chem. **34** (1900) 495.
35. *Murdande, S. B., J. Pikal, M. J., Shanker, R. M., Bogner, R. H.*, J. Pharm. Sci. **99** (2010) 1254. http://dx.doi.org/10.1002/jps.21903
36. *de Waard, H., Frijlink, H. W., Hinrichs, W. L. J.*, Pharm. Res. **28** (2011) 1220. http://dx.doi.org/10.1007/s11095–010–0323–3
37. *Gao, L., Liu, G., Ma, J., Wang, X., Zhou, L., Li, X., Wang, F.*, Pharm Res. **30** (2013) 307. http://dx.doi.org/10.1007/s11095–012–0889-z